Probing neutron-proton asymmetry dependence of source temperature with light charged particles

Y. Huang(黄宇),[1] W. Lin(林炜平),[1] H. Zheng(郑华),[2] R. Wada,[3,4] X. Liu(刘星泉),[1,*] G. Qu(曲国峰),[1] M. Huang(黄美容),[5] P. Ren(任培培),[1] J. Han(韩纪锋),[1] M.R.D. Rodrigues,[6] S. Kowalski,[7] T. Keutgen,[8] K. Hagel,[3] M. Barbui,[3] A. Bonasera,[3,9] and J.B. Natowitz[3]

[1]*Key Laboratory of Radiation Physics and Technology of the Ministry of Education, Institute of Nuclear Science and Technology, Sichuan University, Chengdu 610064, China*

[2]*School of Physics and Information Technology, Shaanxi Normal University, Xi'an 710119, China*

[3]*Cyclotron Institute, Texas A&M University, College Station, Texas 77843*

[4]*School of Physics, Henan Normal University, Xinxiang 453007, China*

[5]*College of Physics and Electronics information, Inner Mongolia University for Nationalities, Tongliao, 028000, China*

[6]*Instituto de Física, Universidade de São Paulo, Caixa Postal 66318, CEP 05389-970, São Paulo, SP, Brazil*

[7]*Institute of Physics, Silesia University, Katowice, Poland.*

[8]*FNRS and IPN, Université Catholique de Louvain, B-1348 Louvain-Neuve, Belgium*

[9]*Laboratori Nazionali del Sud, INFN, via Santa Sofia, 62, 95123 Catania, Italy*

(Dated: April 3, 2020)

Abstract

The dependence of the nuclear temperature on the source neutron-proton (N/Z) asymmetry was experimentally investigated with the light charged particles (LCPs) generated from thirteen reaction systems with different N/Z asymmetries, ^{64}Zn on ^{112}Sn and ^{70}Zn, ^{64}Ni on ^{112,124}Sn, ^{58,64}Ni, ^{197}Au, ^{232}Th at 40 MeV/u. A rather weak N/Z asymmetry dependence of the source temperature was qualitatively inferred from the extracted N/Z asymmetry dependence of the apparent temperature and that of the relative temperature change by the sequential decay effects with the help of the theoretical simulations. Comparing the present result with those from our previous work and other available experimental results, a weak N/Z asymmetry dependence of nuclear temperature is commonly observed in different independent experiments and with different thermometers, except for the result reported by McIntosh *et al.* [Phys. Lett. **B 719**, 337 (2013)]. The origin of the difference between the conclusion of the former group and that of McIntosh *et al.* was addressed, using statistical multifragmentation model (SMM) simulations.

* E-mail at: liuxingquan@scu.edu.cn

I. INTRODUCTION

The concept of nuclear temperature was introduced about seven decades ago in pioneering works performed by Bethe [1] and Weisskopf [2], to describe the formation and decay of a compound nucleus formed in reactions induced by light projectiles, mostly neutrons [3]. Nuclear temperature was later extended to nuclear reactions [4] and applied for studies about nuclear instabilities and the liquid-gas phase transition in nuclear matter [5, 6]. To experimentally extract temperature information, several nuclear "thermometers" have been proposed based on various experimental observables, i.e, energy spectra [7, 8], momentum fluctuations [9], double isotope yield ratios [10] and excited state populations [11] among others. These nuclear thermometers rely on critical thermodynamic conditions such as chemical and thermal equilibrium. In practical applications, however, non-equilibrium processes or mechanisms in nuclear reactions, such as multi-source emission, emission time difference, secondary decay processes among others [3], may significantly influence the accuracy of the nuclear thermometers and result in significant temperature difference deduced from the different thermometers [12]. In spite of these complications, the thermometers are still applicable and widely used in "dependence" studies of nuclear temperature with specific considerations by characterizing the source and examining sequential decay effects. Among these thermometers, the double isotope ratio thermometer has been used to study thermodynamic properties of fragmenting sources, i.e., temperature as a function of excitation energy [13–16], source (or system) neutron-proton asymmetry [17–20], and fragment emission time [21].

The dependence of nuclear temperature on the source neutron-proton (N/Z) asymmetry, also called isotopic dependence of nuclear temperature, is of interest and has been studied for years, as one may expect crucial information on the N/Z asymmetry dependence of the nuclear forces, the properties of excited nuclei and the postulated nuclear liquid-gas phase transition from these studies [4, 22–24]. However, no certain conclusion has been drawn on the N/Z asymmetry dependence of nuclear temperature in both experiments and theories until now. For instance, Wuenschel *et al.* [9] found that the experimentally deduced temperatures from the proton quadrupole momentum fluctuation thermometer show a rather weak source N/Z asymmetry dependence, whereas McIntosh *et al.* [25] found that the deduced temperatures from the same thermometer are notably higher for relatively proton-richer

systems than those for neutron-richer systems. Later, applying the double isotope ratio thermometers to the same data set, McIntosh *et al.* [17] obtained a weak temperature dependence on the source N/Z asymmetry as well. In theoretical work, some predicted that limiting temperatures, defined as the plateau temperature of the caloric curve, are higher for neutron-poor systems [26], whereas others made the opposite prediction [27–29]. To fully understand the N/Z asymmetry dependence of the nuclear temperature, more experimental and theoretical efforts are required.

In this article, measured light charged particle (LCP) yields from thirteen reaction systems with different N/Z asymmetry were used to investigate the N/Z asymmetry dependence of nuclear temperature. For the present isotope yield measurements, the double isotope ratio thermometer of Albergo *et al.* [10] was adopted to deduce temperature values. As the measured isotope yields are perturbed by sequential decay, the temperature from experimental yields, namely "apparent temperature", may have been significantly altered from that at the freezeout, referred as the "real (source) temperature" in this article. The sequential decay effect on temperature determination was taken into account following the analysis strategy in Ref. [19], which was also used in our previous work [30]. This article is organized as follows. In Sec. II, we briefly describe the experiment and data analysis. In Secs. III and IV, the N/Z asymmetry dependence of the nuclear temperature deduced from measured LCP yields is given and discussed. In Sec. V, a summary is given.

II. EXPERIMENT AND DATA ANALYSIS

The experiment was performed at the K-500 superconducting cyclotron facility at Texas A&M University. ^{64,70}Zn and ^{64}Ni beams were used to irradiate ^{58,64}Ni, ^{112,124}Sn, ^{197}Au and ^{232}Th targets at 40 MeV/u. Data from thirteen reaction systems, ^{64}Zn on ^{112}Sn and ^{70}Zn, ^{64}Ni on ^{112,124}Sn, ^{58,64}Ni, ^{197}Au, ^{232}Th, were analyzed in this work. In the experiment, IMFs were detected by a detector telescope placed at 20° in a spherical scattering chamber. The telescope consisted of four Si detectors with the same size of 5 cm × 5 cm and different nominal thicknesses of 129, 300, 1000, 1000 μm, respectively. All four Si detectors were segmented into four sections and each quadrant had a 5° opening in the polar angle. Telescope signals were taken inclusively as the main trigger for all detected events. In coincidence with IMFs, LCPs were measured using 16 single-crystal CsI(Tl) detectors of 3 cm length

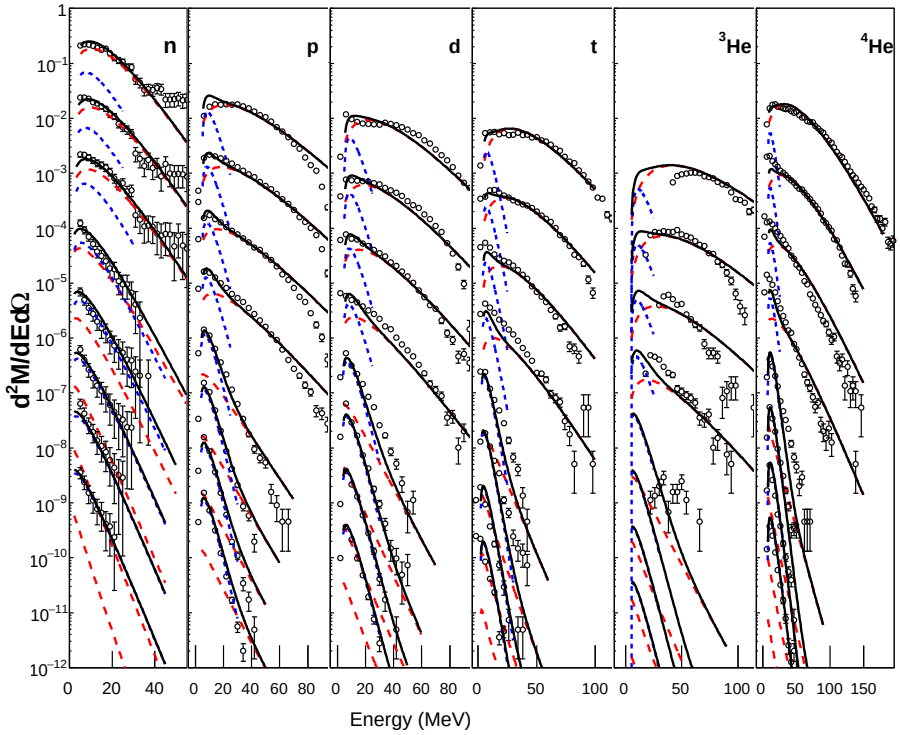

FIG. 1. (Color online) Neutron and light charged particle energy spectra at different θ_{lab} in coincidence with IMFs with $Z \geq 3$ for the ^{64}Ni $+^{112}$ Sn reaction. The differential multiplicity is shown on an absolute scale, but multiplied by a factor of $10^n (n = 0 - 7)$ from the top to the bottom spectra. For neutrons, $\theta_{lab} = 25°, 31°, 40°, 67°, 85°, 104°, 120°, 140°$ and for LCPs, $\theta_{lab} = 36°, 47°, 57°, 70°, 115°, 135°, 145°, 155°$ from top to bottom. Red dashed lines represent the IV source component, blue dotted lines for the TLF source component and the black solid lines for the summation of them.

set around the target at angles between $\theta_{Lab} = 27°$ and $\theta_{Lab} = 155°$. The light output from each detector was read by a photomultiplier tube. The pulse shape discrimination method was used to identify p, d, t, ^{3}He and α particles. The energy calibrations of these particles were performed using Si detectors ($50 \sim 300$ μm) in front of the CsI detectors in separate runs. Sixteen detectors of the Belgian-French neutron detector array DEMON (Detecteur Modulaire de Neutrons) outside the chamber were used to measure neutrons, covering polar angles of $15° \leq \theta_{IMF-n} \leq 160°$ between the telescope and the neutron detectors.

In off-line analyses, simulations of the antisymmetrized molecular dynamics (AMD) [31]

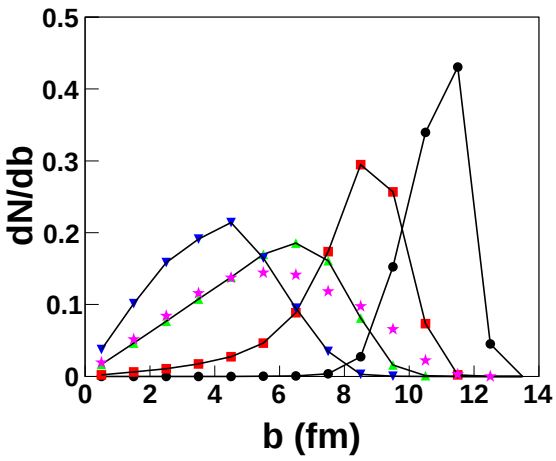

FIG. 2. (Color online) Simulated impact parameter distributions for violent (downward triangles), semi-violent (upward triangles), semi-peripheral (squares) and peripheral (dots) collisions of ^{64}Zn+^{112}Sn at 40 MeV/nucleon. Stars indicate the events in which at least one IMF ($Z \geq 3$) is emitted at 15°-25°. The summed distribution for a given event class is normalized to 1. The figure is taken from Ref. [34].

incorporating with the statistical decay code GEMINI as an afterburner [32] were performed to characterize the measured events. Fig. 2 presents the calculated impact parameter distributions for the system of ^{64}Zn+^{112}Sn at 40 MeV/nucleon. In this figure, the violence of the reaction for each event was determined in the same way as that in Ref. [33], in which the multiplicity of light particles, including neutrons, and the transverse energy of light charged particles were used. The resultant impact parameter distributions for each class of events are shown together with that of the events in which at least one IMF is emitted at the polar angles within 15°-25°. The comparison between the experiment and AMD-GEMINI simulations shown in the figure suggests that the events selected by the inclusive IMF triggers at the polar angles of 15°-25° are corresponding to semi-violent collisions.

To further characterize the fragmenting source to isolate the reaction mechanisms involved in the reaction products, a moving source fit technique [35] was employed. In the moving source fit, the sources were classified as projectile-like (PLF), intermediate-velocity (IV) (also called as nucleon-nucleon-like (NN) [36]), and target-like (TLF) sources according to the source velocity. For neutrons and LCPs, since the measured angles were greater than $\theta_{lab} > 20^o$ where the PLF source component has negligible contributions to the spectra, two sources, the IV source and TLF source, were used in the present moving-source fit. In

the fitting procedures, the IV source was described with a volume type Maxwellian with a velocity around a half beam velocity, whereas the TLF source was described with a surface type Maxwellian with a small source velocity [35]. The Minuit in the Cern library was used to optimize the four parameters for each source, isotope yield, slope parameter, Coulomb energy, and source velocity. Typical fitting results for neutrons, protons, deuterons, tritons, ^{3}He and ^{4}He are shown in Fig. 1 from the left to the right panels, respectively. In the figure, the IV (red dashed lines) and TLF (blue dotted lines) source components dominate in two distinct angular ranges where the IV source component dominates in the top 3-4 spectra whereas the TLF source component dominates in the bottom 3-4 spectra for all cases presented. The parameter errors from the moving source fits were evaluated by performing different optimizations with different initial values within a wide range, rather than by using the errors given by the Minuit which are much smaller in general, because there are many local minima in the present multiple parameter fits. Therefore, large parameter errors (including that of isotope yield) were assigned the multiplicity of the IV source for LCPs. As indicated in Refs. [37, 38], the experimental extraction of nuclear matter properties, such as temperature and density, is strongly influenced by the complicated multi-source emission mechanism. Here, the yields of LCPs from the IV source are used in the following investigation of the N/Z asymmetry dependence of nuclear temperature.

III. RESULTS

1. N/Z asymmetry dependence of apparent temperature

To deduce the nuclear temperature, the double isotope ratio thermometer of Albergo *et al.* [10] was adopted according to the present isotope yield measurements. Under the assumption that chemical equilibrium is established between free nucleons and composite fragments contained within a certain freezeout (fragmentation) volume, the nuclear temperature can be deduced as (see details in Appendix I)

$$T = \frac{B_{diff}}{\ln(aR)}. \tag{1}$$

In this work, two commonly used double isotope ratios, ^{1,2}H/^{3,4}He and ^{2,3}H/^{3,4}He, were applied. The corresponding thermometers are, respectively,

$$T_{^{1,2}H/^{3,4}He} = \frac{18.4}{\ln(5.6R)}, \tag{2}$$

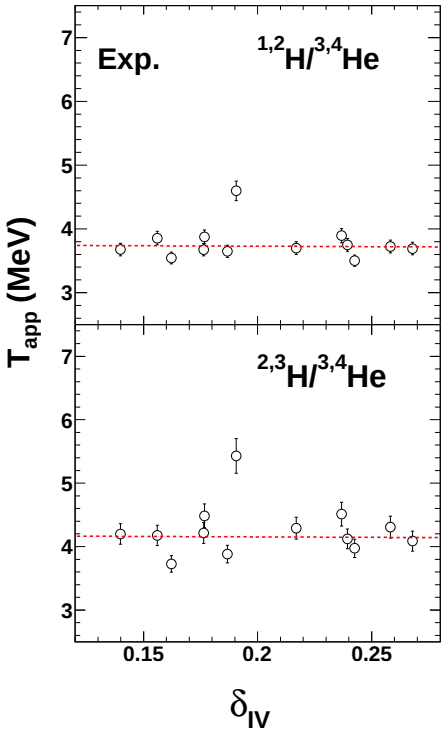

FIG. 3. (Color online) Apparent temperatures from ^{1,2}H/^{3,4}He and ^{2,3}H/^{3,4}He thermometers as a function of source N/Z asymmetry δ_{IV}. Red dashed lines show the global fits with linear functions with one common slope k_{app} and different intercepts.

and

$$T_{^{2,3}H/^{3,4}He} = \frac{14.3}{\ln(1.6R)}. \tag{3}$$

Note that, as the experimental LCP yields which are perturbed by sequential decay are used in Eqs. 2 and 3, the deduced temperature is the "apparent temperature" rather than the "real temperature". In this work, similar to that in our previous work [30], the analysis strategy of Sfienti *et al.* [19] was adopted. That is, instead of using the double isotope thermometer as an absolute thermometer, we used it as a relative thermometer and divide the N/Z asymmetry dependence of the real source temperature into two "parts": one is the N/Z asymmetry dependence of the apparent temperature, T_{app}, and the other is that of the relative temperature change, ΔT, between the apparent and real temperatures due to the sequential decays. The former can be directly determined from the experimental yields, and the latter can be deduced with the aid of theoretical calculations.

The deduced apparent temperature values from ^{1,2}H/^{3,4}He and ^{2,3}H/^{3,4}He thermometers are plotted in Fig. 3 as a function of the IV source N/Z asymmetry, $\delta_{IV} = (N_{IV} - Z_{IV})/A_{IV}$, where N_{IV}, Z_{IV} and A_{IV} are the neutron, proton and mass of the fragmenting source calculated from summing over the experimentally measured IV component yields of neutrons, LCPs and IMFs with $Z \leq 18$. Errors shown in the figure were calculated from the isotope multiplicity errors. As seen in the figure, the apparent temperatures from both thermometers fluctuate around certain mean values, except for one point from the ^{70}Zn+^{64}Ni system, and exhibit almost no dependence on δ_{IV}. The origin of the significant overestimation of the temperature for the ^{70}Zn+^{64}Ni system is unknown, but this data point does not have a significant influence on the overall trend of T_{app} versus δ_{IV}. A global fit to the two T_{app} versus δ_{IV} plots with linear functions with one common slope k_{app} and individual intercepts was performed. The common slope, k_{app}, in the fit reflects the average increasing or decreasing trend of T_{app} as a function of δ_{IV}, whereas the individual intercepts are sensitive to the extracted values of the apparent temperature. From the fit, $k_{app} = -0.1 \pm 0.5$ MeV is obtained, where the error is the fitting error. The obtained k_{app} value is rather small indicating that the apparent temperature decreases slightly as δ_{IV} increases in the presently measured δ_{IV} region, $0.14 \lesssim \delta_{IV} \lesssim 0.27$.

2. N/Z asymmetry dependence of temperature change due to sequential decays

To determine the N/Z asymmetry dependence of nuclear temperature change due to sequential decays, the statistical multifragmentation model (SMM) of Bondorf *et al.* [39] was used. SMM assumes that the fragmentation takes place in equilibrated nuclear matter and the break-up configuration determined by statistical weights. Within the thermodynamic limit, this process is consistent with a possible nuclear liquid-gas phase transition. Here the relative temperature change, ΔT, was defined as the difference between the temperatures from the secondary and primary isotope yields, where the primary fragments were identified as those directly from the fragmentation processes, and the secondary fragments were generated using the default encapsulated sequential decay code as an afterburner. In our previous work [40–42], the symmetry entropy effect was added into the SMM of Bondorf *et al.* and the reconstructed hot fragment yield distributions from the reaction ^{64}Zn + ^{112}Sn at 40 MeV/u were well reproduced by the new SMM. Following analyses are based on the new SMM (referred to "SMM" hereafter).

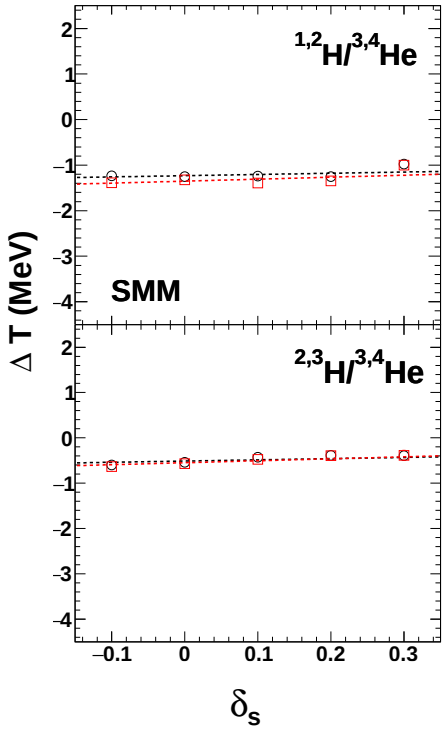

FIG. 4. (Color online) Difference between the temperatures from the secondary and primary isotope yields from the SMM simulations determined using the ^{1,2}H/^{3,4}He and ^{2,3}H/^{3,4}He thermometers as a function of source neutron-proton asymmetry δ_s. Initial fragmentation conditions are E_x/A = 5 MeV and V/V_0=5 (squares), E_x/A = 5 MeV and V/V_0=10 (circles). Dashed lines represent the corresponding global fits with linear functions with one common slope $k_{\Delta T}^{SMM}$ and different intercepts.

In the SMM simulations, fragmenting sources with the same mass number A_s = 100 but different charge numbers, i.e., Z_s = 35, 40, 45, 50 and 55, were used. The source N/Z asymmetry, $\delta_s = 1-2Z_s/A_s$, ranges from -0.1 to 0.3, and fully covers the measured δ_{IV} region. The fragmentation conditions were specified with excitation energies E_x/A =5 MeV and fragmentation volumes V/V_0=5 and 10, where V_0 is the volume with the normal saturation density. The selection of E_x/A =5 MeV corresponds to a fragmentation temperature of ∼5 MeV which has been previously extracted from the IMF yields of the reaction ^{64}Zn+^{112}Sn at 40 MeV/u using a self-consistent method [43]. In Fig. 4, the resultant ΔT versus δ_s relations are plotted for E_x/A = 5 MeV and V/V_0=5 (squares), and E_x/A = 5 MeV and V/V_0=10 (circles). Similar weak dependences of ΔT on the N/Z asymmetry are observed for both thermometers, although the absolute ΔT values are slightly different. This indicates

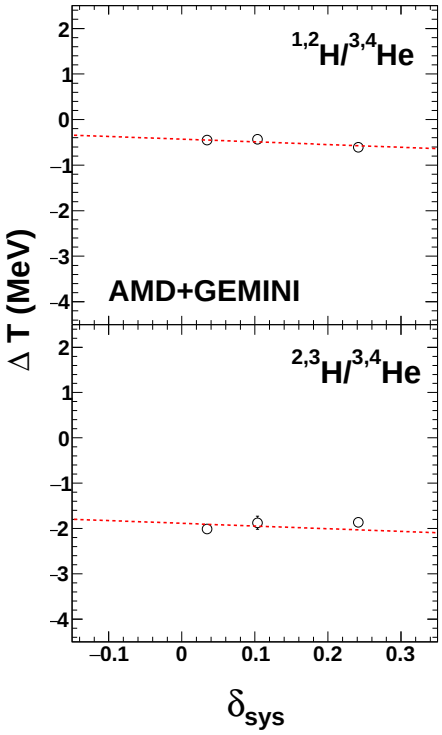

FIG. 5. (Color online) Difference between the temperatures from the secondary and primary isotope yields from the AMD+GEMINI simulations determined using the ^{1,2}H/^{3,4}He and ^{2,3}H/^{3,4}He thermometers as a function of system neutron-proton asymmetry δ_{sys}. Red dashed lines represent the global fits with linear functions with one common slope $k_{\Delta T}^{AMD}$ and different intercepts.

that the nuclear structure characteristics in the secondary decay process is nearly the same for a given double isotope ratio selection among the reaction systems with different N/Z asymmetries, once the initial condition is fixed even if any incomplete inclusion of nuclear structure characteristics is involved. For the results under a given fragmentation condition, the same global fit as that of Fig. 3 was applied, and slopes $k_{\Delta T}^{SMM} = 0.4 \pm 0.2$ MeV for $E_x/A = 5$ MeV and V/V_0=5 (squares) and 0.3 ± 0.2 MeV for $E_x/A = 5$ MeV and V/V_0=10 (circles) are obtained, respectively, where the errors are from the fits. Both $k_{\Delta T}^{SMM}$ values show close agreement and have a consistent magnitude with the deduced $|k_{\Delta T}| \lesssim 2.5$ MeV from the observation reported by Sfienti *et al.* [19], in which the deviation of the secondary decay corrections is less than 300 keV as the N/Z asymmetry changes from 0.07 to 0.19 among the projectile-like fragmenting sources, ^{107}Sn, ^{124}La and ^{124}Sn.

To further clarify the dynamical effect on the N/Z asymmetry dependence of ΔT, simu-

lations of the ^{58}Ti +^{58} Ti, ^{58}Fe +^{58} Fe and ^{58}Ni +^{58} Ni reaction systems at 40 MeV/u, were also performed using the AMD code of Ono *et al.* [31]. For AMD, the dynamical calculation was performed up to 300 fm/c, and the primary fragments from the dynamical process were then de-excited to the ground state using the GEMINI code of Charity *et al.* [32]. Inclusive primary and secondary LCPs from an impact parameter range of 0-8 fm were taken to calculate the real and apparent temperatures, respectively. The resultant ΔT values as a function of system neutron-proton asymmetry δ_{sys} are shown in Fig. 5. Applying the global fit to the ΔT versus δ_{sys} plot from the AMD+GEMINI simulations leads to $k_{\Delta T}^{AMD} = -0.6 \pm 0.4$ MeV. Even though the signs are opposite, the absolute values of $k_{\Delta T}^{SMM}$ and $k_{\Delta T}^{AMD}$ are small, indicating a weak N/Z asymmetry dependence of ΔT. AMD and SMM follow completely different scenarios for the fragment production, that is, AMD is dynamical, whereas SMM is statistical. This consistency suggests an insensitivity of the N/Z asymmetry dependence of ΔT to the fragmentation mechanism and further confirms the weak dependence of the relative temperature change due to sequential decays on the N/Z asymmetry.

3. N/Z asymmetry dependence of real temperature

From the weak N/Z asymmetry dependence of the apparent temperature deduced from the experimental LCP yields with $k_{app} = -0.1 \pm 0.5$ MeV and the weak N/Z asymmetry dependence of the relative temperature change deduced from the theoretical predictions with $k_{\Delta T}^{SMM} = 0.3 \sim 0.4 \pm 0.2$ MeV and $k_{\Delta T}^{AMD} = -0.6 \pm 0.4$ MeV, one can conclude that a change of 1 unit in source N/Z asymmetry corresponds to a maximum absolute change in real temperature by about 0.5 MeV. Therefore, a weak N/Z asymmetry dependence of the real source temperature is inferred. We note that the source mass has a negligible contribution to this result, since no significant size dependence was experimentally observed for the reactions with system sizes and incident energies similar to those of this work [21]. The present weak N/Z asymmetry dependence of temperature deduced from LCP thermometers is rather consistent with that from IMF thermometers in our previous work [30]. This consistency is an indication for early chemical equilibrium prior to the source fragmentation, as LCPs and IMFs involve different emission time scales in the collisions [44, 45]. To fully address this issue, on the other hand, nuclear density information during fragment emission is still required.

IV. DISCUSSION

Detailed comparisons about the available experimental results and ours from IMF yields are given in the previous work [30]. Since the present result is similar to that in the previous work, the comparisons presented in Ref. [30] are valid. From those comparisons, one may find that a weak N/Z asymmetry dependence of nuclear temperature is commonly observed in different reactions and with different thermometers [9, 17, 19, 20], except for the result reported by McIntosh *et al.* [25]. Since Wuenschel *et al.* and McIntosh *et al.* used the same proton quadrupole momentum fluctuation thermometer as a probe, we focus in this article on pursuing the origin of the different result of McIntosh *et al.* [25] by comparing with that of Wuenschel *et al.* [9]. To address the difference, we first briefly describe their analyses and conclusions.

1. Wuenschel *et al.* measured the temperature (caloric curve) of reconstructed quasi-projectiles (QPs) from the reactions of ^{86,78}Kr +^{64,58} Ni at 35 MeV/nucleon collected with the NIMROD-ISiS array housed inside the TAMU Neutron Ball [46]. Charged particle yields were obtained using the Si-CsI telescopes in NIMROD-ISiS. Free neutron yields were provided by the Neutron Ball in conjunction with the event reconstruction with isotopically resolved charged particles. The reconstructed QP source was constrained to be in the QP charge range of Z_{QP}=30-34. The fragments in an accepted event were then cut on the longitudinal velocity relative to that of the largest fragment. The average neutron-corrected N/Z asymmetries of the QPs obtained from the ^{86}Kr +^{64} Ni and ^{78}Kr +^{58} Ni systems were 0.14 and 0.06, respectively [47]. The excitation energies per nucleon of the QPs were from 1.5 MeV to 8.5 MeV. A weak N/Z asymmetry dependence in good agreement with our present result was concluded.

2. McIntosh *et al.* performed their experiment using the same detector array, NIMROD-ISiS and Neutron Ball. The temperature of the reconstructed QPs from the reactions of ^{70}Zn +^{70} Zn, ^{64}Zn +^{64} Zn and ^{58}Ni +^{58} Ni at 35 MeV/nucleon was deduced. The mass of the reconstructed QPs was constrained to be $48 \leq A_{QP} \leq 52$. To select QPs that were equilibrated, it was also required that the emission of the QPs should be spherical on average. The N/Z asymmetries of the reconstructed QPs ranged from 0.04 to 0.24. The excitation energies per nucleon of the QPs were from 2.5 MeV to 8.5 MeV. A significant N/Z asymmetry dependence on the source temperature was concluded, that an increase in

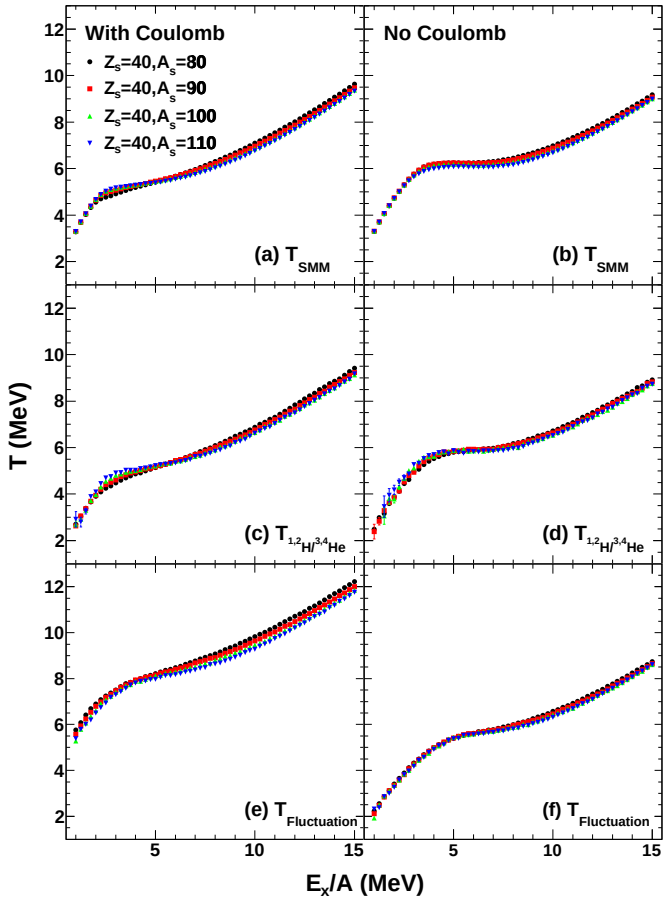

FIG. 6. (Color online) Temperature values as a function of excitation energy per nucleon from SMM calculations with fragmenting sources with the same charge number Z_s=40 and different mass numbers A_s=80, 90, 100, and 110. Left panels are those from SMM calculations that include the Coulomb effects, whereas right panels are those SMM calculations without the Coulomb effect. Upper, middle and lower panels correspond to different temperature determinations. Temperatures in the upper panels are those directly from the SMM, T_{SMM}, and those in the middle and lower panels are deduced using the ^{1,2}H/^{3,4}He thermometer, $T_{^{1,2}H/^{3,4}He}$, and the proton momentum fluctuation thermometer, $T_{fluctuation}$.

N/Z asymmetry of 0.15 unit corresponds to a decrease in fluctuation temperature on the order of 1 MeV.

Wuenschel *et al.* reconstructed the QPs with a constraint on the charge number Z_{QP}, whereas McIntosh *et al.* reconstructed the QPs with a constraint on the mass number A_{QP}. As a consequence, the reconstructed QPs of Wuenschel *et al.* were with similar Z_{QP} but

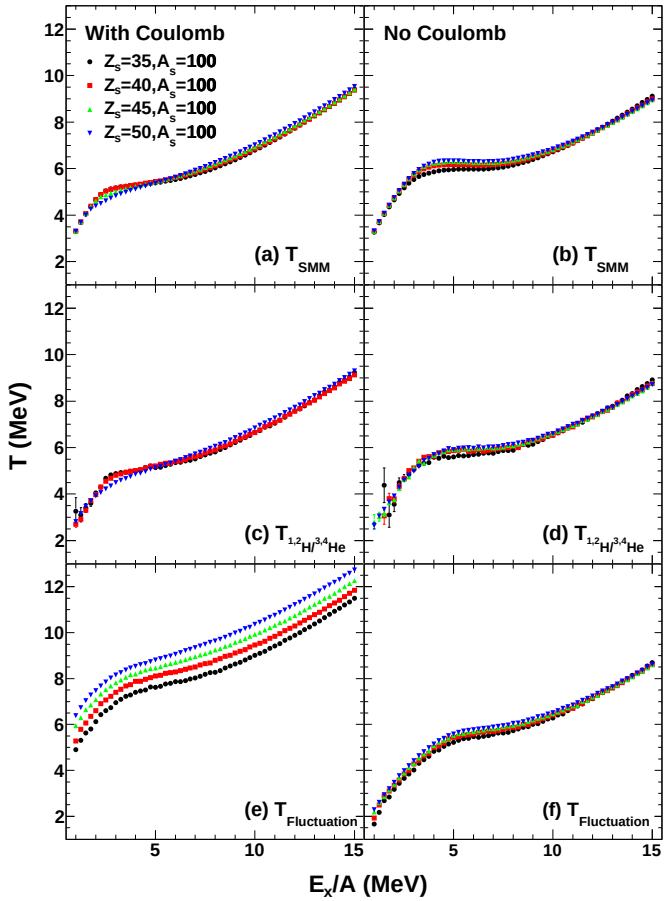

FIG. 7. (Color online) Similar plots to those shown in Fig. 6 but from the SMM calculations with fragmenting sources with the same mass number A_s=100 and different mass numbers Z_s=35, 40, 45, and 50.

different A_{QP}, whereas those of McIntosh *et al.* were with similar A_{QP} but different Z_{QP}. These different constraints on the QP mass and charge may lead to the difference in the temperature dependence on the N/Z asymmetry deduced by Wuenschel *et al.* and McIntosh *et al.*. It should be mentioned that in some studies, especially in the symmetry energy studies [48, 49], reconstructed sources or systems with the constant mass are commonly used. This is because for the sources with the same mass, the effects from the volume and surface of the sources are eliminated, so that one may isolate the symmetry energy term with the aid of dynamical or statistical calculations without a Coulomb term.

To clarify the effect of the different constraints, additional SMM simulations were performed besides those in Sec.III.2 where the fragmenting sources have the same charge number

Z_s=40 but different mass numbers A_s=80, 90, 100, and 110. In the additional group of the SMM simulations, the fragmenting sources have the same mass number A_s=100 but different charge numbers Z_s=35, 40, 45, and 50. Two group calculations are essentially corresponding to the two QP reconstruction constraints of Wuenschel *et al.* [47] and McIntosh *et al.* [25], respectively. The source N/Z asymmetries for both groups fully cover the measured QP N/Z asymmetry regions. Fragmentation volume was set as $6V_0$. The excitation energies were in the same range of E_x/A=1-15 MeV with a step of 0.25 MeV, which also fully cover the measurement region. More than 1 million events were generated for each given E_x/A. SMM calculations without the Coulomb force were separately performed under the same initial conditions for comparison. Sequential decay effect in the SMM was ignored, since in the N/Z asymmetry study the thermometers can be used as a relative temperature probe so that the sequential decay effects are not important. Indeed in Ref. [19], the sequential decay effects were examined and no significant effect on the N/Z asymmetry dependence of the source temperature was concluded.

In Fig. 6, temperature values as a function of excitation energy per nucleon for the fragmenting sources with the same Z_s (corresponding to the QP mass constraint of Wuenschel *et al.*) are plotted, where left and right panels represent those from calculations with and without the Coulomb force, respectively. Upper, middle and lower panels correspond to different temperature determinations, where temperatures in the upper panels are the fragmentation (or equilibrium) temperatures calculated from the energy balance in the SMM (T_{SMM}) as references. Those in the middle and lower panels are deduced using the ^{1,2}H/^{3,4}He thermometer, $T_{^{1,2}H/^{3,4}He}$, and the proton quadrupole momentum fluctuation thermometer, $T_{fluctuation}$, respectively. Different symbols represent the results for the sources with different A_s as indicated in the top-left panel. Error bars are smaller than the data points. From Figs. 6(a)-(f), weak N/Z asymmetry dependences of nuclear temperature are observed for all cases with different temperature determination methods, and with or without the Coulomb effect. These results are consistent with those from our works and those from Kunde *et al.* [20], Sfienti *et al.* [19] and Wuenschel *et al.* [9]. Similar results to those in Fig. 6 but from the SMM calculations with fragmenting sources with the same A_s are presented in Fig. 7, which correspond to the QP mass constraint of McIntosh *et al.*. From Figs. 7(a)-(d), weak N/Z asymmetry dependences of both T_{SMM} and $T_{^{1,2}H/^{3,4}He}$ are also observed both with and without the Coulomb effect. In contrast, the proton momentum fluctuation thermometer

gives a significant N/Z asymmetry dependence of temperature as shown in Fig. 7(e). The increase of 1 unit in δ_s corresponds to a decrease in $T_{fluctuation}$ on an average order of 5-6 MeV in the overall excitation energy region, in good agreement with the result of McIntosh *et al.* [25]. After turning off the Coulomb force in the SMM, however, the significant N/Z asymmetry dependence of $T_{fluctuation}$ disappears as shown in Fig. 7(f). This fact strongly indicates a close correlation between the significant N/Z asymmetry dependence of temperature obtained by McIntosh *et al.* and the Coulomb effect.

In the SMM, fragmentations are constrained by the conservation of mass, charge, momentum, and energy. The collective radial motion of the fragments from the Coulomb force is superimposed upon the internal random thermal motion. As a consequence of the superposition of the radial collective motion (expansion) on the thermal motion, the deduced quadrupole momentum fluctuation temperature becomes larger in sources with larger Z_s, in which the Coulomb effect is more significant. This results in the significant dependence of $T_{fluctuation}$ on the source N/Z asymmetry in Fig. 7(e). In the case of Fig. 6(e), since the Coulomb contributions among the sources with different N/Z asymmetries are almost equal due to the same given Z_s, the significant dependence of $T_{fluctuation}$ on the source N/Z asymmetry disappears. To further investigate the Coulomb effect, we applied the classical Coulomb correction of Ref. [50] to the $T_{fluctuation}$ values in panels (e) of Figs. 6 and 7. The corrected temperature ($T_{Corr.}$) values as a function of E_x/A are shown in Fig. 8. Upper and lower panels correspond to results from sources with the same Z number and the same A number, respectively. It is found that the Coulomb correction reduces the absolute temperature values significantly, that is, the $T_{Corr.}$ values in both panels become significantly smaller and similar to those of T_{SMM} in Figs. 6(a) and 7(a), though their values are still around 1-2 MeV higher in the overall E_x/A region. One also may notice that for the case with the same A number (lower panel), the offset of the temperature N/Z dependence remains, but significantly reduces comparing to that in Fig. 7(e). In the SMM, the Coulomb energy creates a radial expansion flow under a simultaneous multifragmentation scenario, whereas the Coulomb correction of Zheng *et al.* [50] is made for the acceleration of the probe particle in the source Coulomb field alone, and thus the Coulomb correction in the latter is only partial. Therefore the above observed differences originate from the incomplete inclusion of the collective radial flow before the Coulomb acceleration in the Coulomb correction. From the above comparisons, we conclude that the significant N/Z dependence of the source tempera-

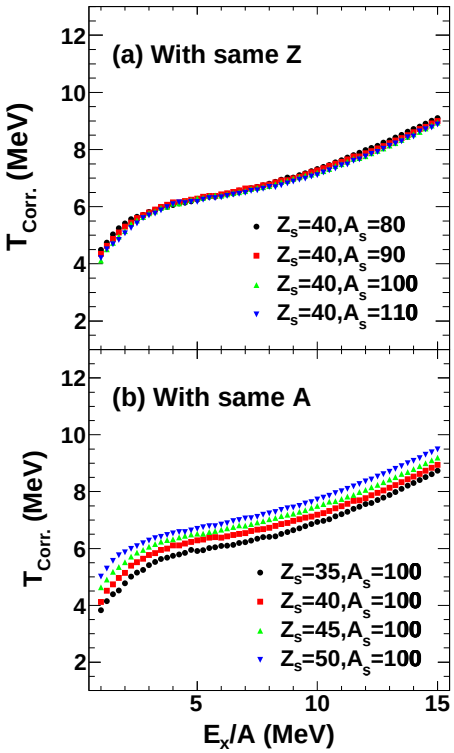

FIG. 8. (Color online) Similar plots to those in panels (e) of Figs. 6 and 7 but with the Coulomb correction of Ref. [50]. Upper and lower panels are corresponding to the results from sources with the same Z number and the same mass number, respectively.

ture observed by McIntosh *et al.* originates from the different Coulomb contributions in the reconstructed QPs with different charges under the QP mass constraint. On the other hand, since the double isotope ratio temperature is dominated by the chemical equilibrium during fragmentations (commonly assumed in SMM simulations) rather than the Coulomb force, the double isotope ratio temperature shows a weak source N/Z asymmetry dependence for both cases with and without the Coulomb force.

Apart from the absolute values, the shapes of $T_{^{1,2}H/^{3,4}}$ versus E_x/A and $T_{fluctuation}$ versus E_x/A are similar to that of T_{SMM} versus E_x/A in Fig. 9(a), in which the results of $Z_s = 45$ in Fig. 7(a),(c) and (e) are depicted. This fact indicates an applicability in deducing the critical behavior of hot nuclear matter using both ^{1,2}H/^{3,4}He thermometer and proton momentum fluctuation thermometer. After sequential decays, however, the temperature values and their trends as a function of E_x/A from both the ^{1,2}H/^{3,4}He thermometer and the proton momentum fluctuation thermometer are significantly altered and become quite different from

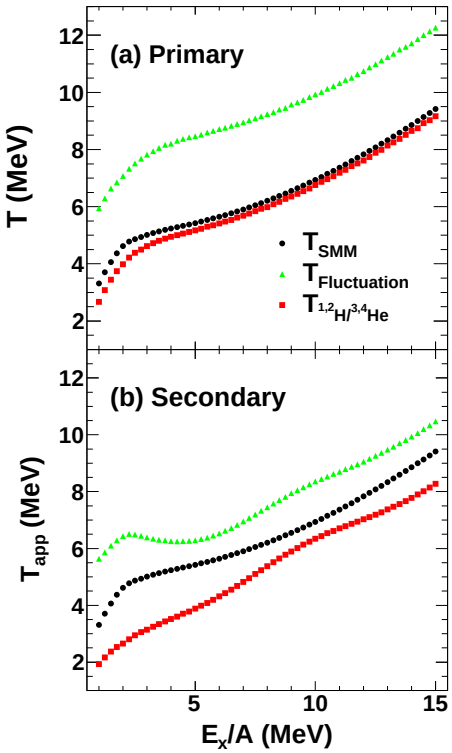

FIG. 9. (Color online) Temperature values as a function of excitation energy per nucleon for the $Z_s = 45$ source. Upper and lower panels correspond to the results from primary hot fragments and secondary cool fragments. Different symbols represent different temperatures, T_{SMM} (dots), $T_{^{1,2}H/^{3,4}He}$ (squares), and $T_{fluctuation}$ (triangles). The same T_{SMM} is plotted in both upper and lower panels as a reference.

those of the primary yields, as shown in Fig. 9(b). This indicates that careful treatment of the sequential decay effects are important to study the behavior of the hot nuclear matters using the double isotope ratio thermometer and the quadrupole momentum fluctuation thermometer.

V. SUMMARY

The N/Z asymmetry dependence of the nuclear temperature was experimentally investigated with the yields of the LCP isotopes produced from thirteen reaction systems with different N/Z asymmetries, ^{64}Zn on ^{112}Sn and ^{70}Zn, ^{64}Ni on ^{112,124}Sn, ^{58,64}Ni, ^{197}Au, ^{232}Th at 40 MeV/nucleon. The apparent temperatures for these systems were determined from the measured LCP yields from the IV sources using the ^{1,2}H/^{3,4}He and ^{2,3}H/^{3,4}He thermome-

ters. A rather weak N/Z asymmetry dependence of the extracted apparent temperature is observed in the measured source N/Z asymmetry range in the present study. To take into account the alteration of the measured isotope yields by the sequential decay processes, the N/Z asymmetry dependence of the relative temperature change, which was defined as the difference between the temperatures from the secondary and primary isotope yields, was investigated using the SMM and AMD+GEMINI simulations. The real source temperature was then qualitatively inferred to have a rather weak dependence on the source N/Z asymmetry from the deduced N/Z asymmetry dependence of the apparent temperature and the relative temperature change. The present result was compared with those from our previous work and other independent experiments. A weak N/Z asymmetry dependence of nuclear temperature is commonly observed from different independent experiments and with different thermometers, except for the result reported by McIntosh *et al.* [25]. With close examinations of the experimental details of Wuenschel *et al.* and McIntosh *et al.* and combining with SMM simulations, we conclude that the significant N/Z dependence of the source temperature observed by McIntosh *et al.* originates from the Coulomb contribution difference in the reconstructed QPs with different charges under the QP mass constraint.

ACKNOWLEDGEMENT

The authors thank the operational staff in the cyclotron Institute, Texas A&M University, for their support during the experiment. The authors thank A. Ono for providing his code. This work was supported by the National Natural Science Foundation of China (No. 11705242, U1632138, 11805138, 11905120, 11775273, 11575269, 11775013), the Fundamental Research Funds For the Central Universities (No. YJ201954, YJ201820 and GK201903022) in China, the CAS Pioneer Hundred Talents Program and the National MCF Energy R&D Program of China (No. 2018YFE0310200). This work was also supported by the US Department of Energy under Grant No. DE-FG02-93ER40773 and the Robert A. Welch Foundation under Grant A330.

[1] H.A. Bethe, Rev. Mod. Phys. **9**, 69 (1937).

[2] V.F. Weisskopf, Phys. Rev. **52**, 295 (1937).

[3] A. Kelić, J.B. Natowitz and K.-H. Schmidt, Eur. Phys. J. **A 30**, 203(2006).

[4] E. Suraud, Ch. Grégoire, B. Tamain, Prog. Part. Nucl. Phys. **23**, 357 (1989).

[5] D.H.E. Gross, Rep. Prog. Phys. **53**, 605 (1990).

[6] J.P. Bondorf *et al.*, Phys. Rep. **257**, 133 (1995).

[7] G. D. Westfall *et al.*, Phys. Lett. **B 116** 118, (1982).

[8] B. V. Jacak *et al.*. Phys. Rev. Lett. **51**, 1846 (1983).

[9] S. Wuenschel *et al.*, Nucl Phys **A 843**, 1, (2010).

[10] S. Albergo *et al.* Nuovo Cimento **A 89**, 1, (1985).

[11] D. J. Morrissey *et al.*, Phys. Lett. **B 148**, 423 (1984).

[12] C. Guo and F. Zhang, Nucl. Sci. and Tech. **24**, 050513 (2013).

[13] J.B. Natowitz *et al.*, Phys. Rev. **C 65**, 034618 (2002).

[14] W. Trautmann *et al.*, Phys. Rev. **C 76**, 064606 (2007).

[15] H.F. Xi *et al.*, Phys. Rev. **C 58**, 2636 (1998) (R).

[16] V. Serfling *et al.*, Phys. Rev. Lett. **80**, 3928 (1998).

[17] A.B. McIntosh *et al.*, Phys. Rev. **C 87**, 034617 (2013).

[18] W. Trautmann *et al.*, Int. J. Mod. Phys. **E 17**, 1838 (2008).

[19] C. Sfienti *et al.*, Phys. Rev. Lett. **102**, 152701 (2009).

[20] G.J. Kunde *et al.*, Phys. Lett **B 416**, 56 (1998).

[21] J. Wang *et al.*, Phys. Rev. **C 72**, 024603 (2005).

[22] W. A. Friedman, Phys. Rev. Lett. **60**, 2125 (1988).

[23] D. Gross *et al.*, Prog. Part. Nucl. Phys. **30**, 155 (1993).

[24] Bao-An Li, Lie-Wen Chen, and Che Ming Ko, Phys. Rep. **464**, 113 (2008).

[25] A.B. McIntosh *et al.*, Phys. Lett. **B 719**, 337 (2013).

[26] C. Hoel, L.G. Sobotka, R.J. Charity, Phys. Rev. **C 75**, 017601 (2007).

[27] J. Besprosvany, S. Levit, Phys. Lett. **B 217**, 1 (1989).

[28] R. Ogul, A.S. Botvina, Phys. Rev. **C 66**, 051601 (2002)(R).

[29] J. Su, F.S. Zhang, Phys. Rev. **C 84**, 037601 (2011).

[30] X. Liu *et al.*, Phys. Rev. **C 100**, 064601 (2019).

[31] A. Ono, Phys. Rev. **C 59**, 853 (1999).

[32] R.J. Charity *et al.*, Nucl. Phys. **A 483**, 371 (1988).

[33] R. Wada *et al.*, Phys. Rev. **C 69**, 044610 (2004).

[34] M. Huang *et al.*, Phys.Rev. **C 82**, 054602 (2010).

[35] T.C. Awes, G. Poggi, C.K. Gelbke *et al.*, Phys. Rev. **C 24**, 89 (1981).

[36] Z. Chen *et al.*, Phys.Rev. **C 81**, 064613 (2010).

[37] M.B. Tsang *et al.*, Phys. Rev. Lett. **92**, 062701 (2004).

[38] H.S. Xu *et al.*, Phys. Rev. Lett. **85**, 716 (2000).

[39] J. Bondorf *et al.*, Phys. Rep. **257**, 133 (1995).

[40] W. Lin *et al.*, Phys. Rev. **C 97**, 044603 (2018).

[41] W. Lin *et al.*, Phys. Rev. **C 97**, 054615 (2018).

[42] W. Lin *et al.*, Phys. Rev. **C 99**, 054616 (2019).

[43] X. Liu *et al.*, Phys. Rev. **C 90**, 014605 (2014).

[44] F.Z. Ighezou *et al.*, Nucl. Phys. **A 662**, 295 (2000).

[45] L. Beaulieu *et al.*, Phys. Rev. Lett. **84**, 5971 (2000).

[46] S. Wuenschel *et al.*, Nucl. Instrum. Methods Phys. Res. **A 604**, 578 (2009).

[47] S. Wuenschel *et al.* Phys. Rev. **C 79**, 061602 (2009)(R).

[48] G. Giuliani, H. Zheng and A. Bonasera, Prog. Part. Nucl. Phys. **76**, 116 (2014).

[49] D.V. Shetty *et al.*, Phys. Rev. **C 76**, 024606 (2007).

[50] H. Zheng, G. Giuliani and A. Bonasera, J. Phys. G: Nucl. Part. Phys. **41**, 055109 (2014).

APPENDIX I

Under the assumption that equilibrium may be established between free nucleons and composite fragments contained within a certain freezeout volume V and a temperature T, the density of an isotope with A nucleons and Z protons (A, Z) may be expressed as

$$\rho(A,Z) = \frac{N(A,Z)}{V} = \frac{A^{3/2}\cdot\omega(A,Z)}{\lambda_T^3}\cdot\exp\left[\frac{\mu(A,Z)}{T}\right], \tag{4}$$

where $N(A, Z)$ is the number of isotope (A, Z) within the volume V; $\lambda_T = h/(2\pi m_0 T)^{1/2}$ is the thermal nucleon wave-length, where m_0 is the nucleon mass; $\omega(A, Z)$ is the internal partition function of the isotope (A, Z) and related to the ground- and excited-state spins (practically, $\omega(A, Z)$ is limited to that at the ground state [10]); $\mu(A, Z)$ is the chemical potential of the isotope (A, Z). In chemical equilibrium, $\mu(A, Z)$ is expressed as

$$\mu(A,Z) = Z\mu_p + (A-Z)\mu_n + B(A,Z), \tag{5}$$

where $B(A,Z)$ is the binding energy of the isotope (A,Z). μ_p and μ_n are the chemical potentials of free protons and free neutrons, respectively. Calculating the densities of free protons and neutrons, ρ_p and ρ_n, in the same volume using Eqs. 4 and 5, performing transforms to obtain μ_p and μ_n, and then inserting μ_p and μ_n back into Eq. 4, one obtains,

$$\rho(A,Z) = \frac{N(A,Z)}{V} = \frac{A^{3/2}\cdot\omega(A,Z)\cdot\lambda_T^{3(A-1)}}{(2s_p+1)^Z\cdot(2s_n+1)^{A-Z}}\cdot\rho_p^Z\cdot\rho_n^{A-Z}\exp\left[\frac{B(A,Z)}{T}\right], \tag{6}$$

where s_p and s_n are the spins of the free proton and neutron, respectively. The ratio between the measured yields of two different isotopes is then

$$\frac{Y(A,Z)}{Y(A',Z')} = \frac{\rho(A,Z)}{\rho(A',Z')} = \left(\frac{A}{A'}\right)^{3/2}\left(\frac{\lambda_T^3}{2}\right)^{A-A'}\frac{\omega(A,Z)}{\omega(A',Z')}\rho_p^{(Z-Z')}\rho_n^{(A-Z)-(A'-Z')} \cdot\exp\left[\frac{B(A,Z)-B(A',Z')}{T}\right], \tag{7}$$

The free proton density can be calculated from the yield ratio of two fragments with only one proton difference, such as (A,Z) and $(A+1,Z+1)$,

$$\rho_p = C\cdot\left(\frac{A}{A+1}\cdot T\right)^{3/2}\frac{\omega(A,Z)}{\omega(A+1,Z+1)}\cdot\exp\left[\frac{B(A,Z)-B(A+1,Z+1)}{T}\right]\cdot\frac{Y(A+1,Z+1)}{Y(A,Z)}, \tag{8}$$

where C is the constant related to the unit conversion. Analogously, the free neutron density is calculated from the yield ratio of two fragments with only one neutron difference, such as (A,Z) and $(A+1,Z)$,

$$\rho_n = C\cdot\left(\frac{A}{A+1}\cdot T\right)^{3/2}\frac{\omega(A,Z)}{\omega(A+1,Z)}\cdot\exp\left[\frac{B(A,Z)-B(A+1,Z)}{T}\right]\cdot\frac{Y(A+1,Z)}{Y(A,Z)}. \tag{9}$$

For a given temperature T, the same free proton (or neutron) density must be evaluated from Eq. 8 (or 9). Choosing two ratios with one proton (or neutron) excess, one can deduce the relation between T and the experimental yield ratios as

$$T = \frac{B_{diff}}{\ln(aR)}, \tag{10}$$

and the error of T, δT, is deduced as

$$\delta T = \frac{B_{diff}}{\ln^2(aR)}\cdot\frac{\delta R}{R}, \tag{11}$$

where $R = (Y_1/Y_2)/(Y_3/Y_4)$ is the double isotope yield ratio of the ground states for isotope pairs $(1,2)$ and $(3,4)$, and δR is the error of R. One can find from Eq. 11 that δT depends

on both $B_{diff}/\ln^2(aR)$ and $\delta R/R$. For the $(1,2)$ and $(3,4)$ ratios with same one-neutron excess used this work, B_{diff} is the binding energy difference, $B_{diff} = (B_1 - B_2) - (B_3 - B_4)$, and a is the statistical weighting factor and is defined as

$$a = \frac{\omega_3/\omega_4}{\omega_1/\omega_2}\left[\frac{A_3/A_4}{A_1/A_2}\right]^{1.5}, \tag{12}$$

where $\omega_i = 2S_i + 1$ and S_i is the ground state spin of the ith isotope and A_i is the mass number of the ith isotope.